

Article

A Study on the Effectiveness of Partial Discharge Models for Various Electrical Machines' Insulation Materials

Dimosthenis Verginadis ¹, Tryfon Iakovidis ¹, Athanasios Karlis ^{1,*}, Michael Danikas ¹
and Jose-Alfonso Antonino-Daviu ²

¹ Department of Electrical & Computer Engineering, Democritus University of Thrace (DUTH), 671 00 Xanthi, Greece

² Instituto Tecnológico de la Energía, Universitat Politècnica de València, 46022 Valencia, Spain

* Correspondence: akarlis@ee.duth.gr

Abstract: A vital component of electrical machines (EMs), which plays the most significant role in their reliable and proper operation, is their insulation system. Synchronous generators (SGs) are the most commonly used EMs in energy production and industry. Epoxy resin and mica are the predominant insulation materials for the SGs' windings because their characteristics and properties are suitable for extending the lifetime of the insulation. Partial discharges (PDs) are both a symptom of insulation degradation, as they cause serious problems for insulation, and a means to identify possible insulation faults with offline and/or online PD tests and measurements. A comparison of three different equivalent circuit models of PDs occurring in different insulation materials (epoxy resin, mica, and a combination of these two) is presented in this paper. Different applied voltages and/or various geometries of voids are the factors investigated through simulations. The number of PDs, PD activity, and flashover voltages are examined in order to evaluate which of the aforementioned materials has the best reaction against PD activity.

Keywords: capacitive model; electrical machines; epoxy resin; flashover voltage; insulation system; mica; MATLAB/Simulink; partial discharges; partial discharge model; synchronous generators



Citation: Verginadis, D.; Iakovidis, T.; Karlis, A.; Danikas, M.; Antonino-Daviu, J.-A. A Study on the Effectiveness of Partial Discharge Models for Various Electrical Machines' Insulation Materials. *Machines* **2023**, *11*, 230. <https://doi.org/10.3390/machines11020230>

Academic Editors: Antonio J. Marques Cardoso, Dan Zhang, Giuseppe Carbone and Alejandro Gómez Yepes

Received: 28 December 2022

Revised: 1 February 2023

Accepted: 2 February 2023

Published: 4 February 2023



Copyright: © 2023 by the authors. Licensee MDPI, Basel, Switzerland. This article is an open access article distributed under the terms and conditions of the Creative Commons Attribution (CC BY) license (<https://creativecommons.org/licenses/by/4.0/>).

1. Introduction

A synchronous generator (SG) is one of the most used electrical machines (EMs) in energy production, the industry, and high-kW applications. Besides its high efficiency, its reliable and proper operation as well as maximum performance with minimum maintenance are the main characteristics of an SG [1].

An SG's insulation system, which, most of the time, consists of a combination of epoxy resin (ER) and mica, should avoid possible faults; thus, it plays a crucial role on preserving all the aforementioned characteristics. ER is widely used for adhesive purposes, and its molecular formula is $C_{21}H_{25}ClO_5$ [2]. It has high mechanical strength and chemical resistance and good physical and electrical properties, and it is resistant to moisture and radiation. Mica has low dielectric losses and good mechanical resistance, dielectric constant, and thermal conductivity. The combination of these two insulation materials creates very good insulation properties for SGs [3–5].

Partial discharges (PDs) [3] are electrical discharges, which partially bridge the insulation between conductors, and they are considered both a symptom and a mechanism of insulation aging. The PD analysis differs in relation to different apparatuses, since PDs are a serious problem for EMs, transformers, and high-voltage (HV) cables [6–9]. Specifically speaking, capacitive models are used for studying enclosed cavities; Pedersen's model proposes the model of induced charge theory and studies PDs in cavities; the finite element method (FEM) is used in order to measure the apparent charge magnitude and to model 3D geometry; numerical models use different formulas for the simulation of PD activity and the insulation system; and artificial intelligence (AI) PD models create algorithms for the

processing and analysis of PD data [4] [9–12]. Reference [6] studies the harmonic voltage on PD properties for the insulation of a DC cable, where the PD model consists of the test object, as well as capacitances and resistances. In [7], the authors use FEM in order to study PD activity for a high-temperature superconducting (HTS) transformer.

This paper compares three different PD models, i.e., the classic capacitive model, a capacitive model with the addition of three resistors, and an advanced capacitive model with a more detailed measuring system. The purpose of this comparison is to determine which of the aforementioned insulation materials has the best reaction against PD activity as well as to highlight the differences between the models.

2. Partial Discharges in Electrical Machines

Every EM has to face thermal, electrical, ambient, and mechanical (TEAM) stresses during its operation and lifetime. Electrical stresses and especially PDs are the faults that most stress the stator winding insulation of a generator [13]. The following figures, which were taken during visual inspection using a borescope, show the stator of a real SG in Greece and the results of corrosion occurrence due to PD activity and electrical stresses.

In Figure 1, traces of PDs and a general degradation of the stator's insulation system are evident. It becomes clear that PDs can cause serious faults in EMs' insulation systems. If a winding fault happens during operation, the consequential damages to the EMs can lead to significant outage times. PD tests and measurements (IEC 60034-27) on rotating machines give the possibility to monitor (periodically or permanently) the condition of the electrical properties of an insulation system so that potential problems can be detected and preventive maintenance can be scheduled during planned outages. During the offline condition of the EM, the PD measurement can reveal the locations in the insulation system with weak dielectric properties. The principle of PD measurement is to measure the pulses, which are generated by charge displacements occurring within or on the stator winding insulation system, and then capture them using PD couplers temporarily connected to the EMs' terminals.



Figure 1. Results from PD activity and electrical stress.

3. PD Models

Three different PD models were created in MATLAB/Simulink (The MathWorks, Inc., Natick, MA, USA) in order to investigate the factors affecting PD activity. Three different insulation materials were used, i.e., ER, mica, and a combination (C) of these two. In order to calculate the relative permittivity of the combination of the two insulation materials, the following formula was used [14]:

$$e_{r3} = \frac{e_{r1}e_{r2}(s_1 + s_2)}{e_{r1}s_2 + e_{r2}s_1} \quad (1)$$

where $e_{r1} = 5$ is the relative permittivity of mica, $e_{r2} = 3.6$ is the relative permittivity of ER, s_1 is the width of mica, and s_2 is the width of ER. Moreover, ER and mica were supposed to cover the same volume of the test object. The relative permittivity of the combination of these two insulation materials was calculated as $e_{r3} = 4.12$.

Furthermore, three different applied voltages (5 kV, 10 kV, and 15 kV) were taken into consideration. The dimensions of the test object were 40 mm × 20 mm × 40 mm, while the dimensions of a cylindrical void inside the insulation material were considered to be radius $r = 6$ mm and height $h = 16$ mm. Simulations were also made with double the radius and double the height of the cylindrical void. Indicative samples of the simulation results chosen from each model are presented here because of lack of space.

3.1. Capacitive Model

The capacitive model is an equivalent circuit of three capacitors, which was first presented by Gemant and Philipoff in 1932, and since then many different proposals have been made to improve this model. Figure 2 presents the capacitive model created in MATLAB/Simulink, the elements of which are presented in Table 1 [3].

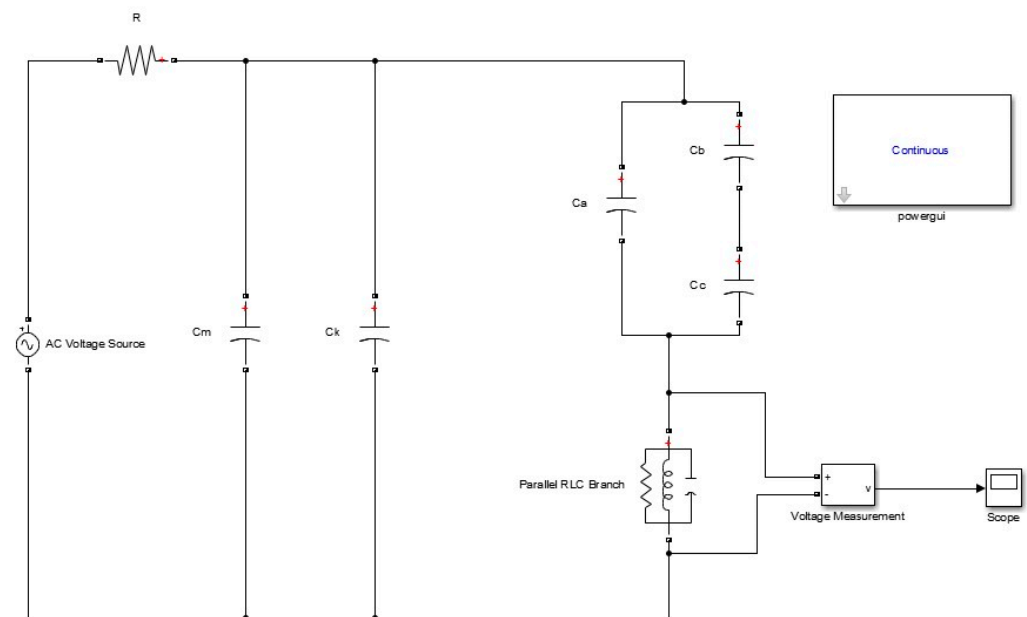


Figure 2. Capacitive model.

Table 1. Capacitive Model's Parameters.

Parameter	Value
Ac High-Voltage (HV) Source	5 kV, 10 kV, 15 kV
Resistor (R_1)	1000 Ω
HV Measuring Capacitor (C_m)	1000 pF
Coupling Capacitor (C_k)	10 μ F
R_m	50 Ω
C_m	0.45 μ F
L_m	0.6 mH

The parameters of this model are [15]:

- Resistor (R_1), acting as a HV filter in order to reduce the noise of the source;
- HV measuring capacitor and coupling capacitor, used in order to capture the displacement current created during PD;
- R_m , C_m and L_m , consisting of the measuring impedance (MI);
- Three capacitors (C_a , C_b , C_c), whose values depend on the insulation material and are calculated by:

$$C_a = \frac{\varepsilon_0 \varepsilon_r (a - 2r)b}{d} \quad (2)$$

$$C_b = \frac{\varepsilon_0 \varepsilon_r r^2 \pi}{d - h} \quad (3)$$

$$C_c = \frac{\varepsilon_0 r^2 \pi}{h} \quad (4)$$

where ε_0 is the dielectric constant in vacuum; ε_r is the relative permittivity (dielectric constant) of the insulating material; a is the length, b is the weight, and d is the height of the test object; and r is the radius and h is the height of the void. It must be noted that C_c is the capacitance of the void in the solid, C_b is the capacitance of the insulation material connected to the void, and C_a is the capacitance of the remaining insulation. Table 2 presents the values for the three capacitors used for the initial simulations, while Tables 3 and 4 show the values for the simulations with doubled radius and doubled height, respectively. In the case of the doubled radius, there is a reduction in C_a and an increase in C_b and C_c , while in the case of doubled height, C_a has the same value, C_b increases, and C_c decreases. Moreover, C_c is the same for all insulation materials. Mica has the highest values for all capacitors, while ER the lowest. The combination of these two insulation materials gives different values.

Table 2. Capacitive Model's Parameters (h, r).

Parameter	Value—ER	Value—Mica	Value—C
C_a	$4.4624 * 10^{-13}$ F	$7.4373 * 10^{-13}$ F	$5.5780 * 10^{-13}$ F
C_b	$1.5012 * 10^{-13}$ F	$2.5021 * 10^{-13}$ F	$1.8766 * 10^{-13}$ F
C_c	$6.2553 * 10^{-14}$ F	$6.2553 * 10^{-14}$ F	$6.2553 * 10^{-14}$ F

Table 3. Capacitive Model's Parameters (h, 2 r).

Parameter	Value—ER	Value—Mica	Value—C
C_a	$2.5499 * 10^{-13}$ F	$4.2499 * 10^{-13}$ F	$3.1874 * 10^{-13}$ F
C_b	$6.0051 * 10^{-13}$ F	$10.0085 * 10^{-13}$ F	$7.5064 * 10^{-13}$ F
C_c	$2.5021 * 10^{-13}$ F	$2.5021 * 10^{-13}$ F	$2.5021 * 10^{-13}$ F

Table 4. Capacitive Model's Parameters (2 h, r).

Parameter	Value—ER	Value—Mica	Value—C
C_a	$4.4624 * 10^{-13}$ F	$7.4373 * 10^{-13}$ F	$5.5780 * 10^{-13}$ F
C_b	$4.5038 * 10^{-13}$ F	$7.5064 * 10^{-13}$ F	$5.6298 * 10^{-13}$ F
C_c	$3.1276 * 10^{-14}$ F	$3.1276 * 10^{-14}$ F	$3.1276 * 10^{-14}$ F

Various results for each insulation material and different geometries of the cylindrical void are indicatively presented in Figures 3–11, where the flashover voltages (FVs) per time are shown. The following diagrams show that the geometry of the enclosed void as well as the applied voltage play a vital role in PD activity, i.e., when the aforementioned factors increase, the number of PDs increases as well. Another factor examined is the insulation materials, and it is obvious that the combination of the two insulation materials has the lowest number of PDs, while mica has more PDs and a smaller maximum PD amplitude.

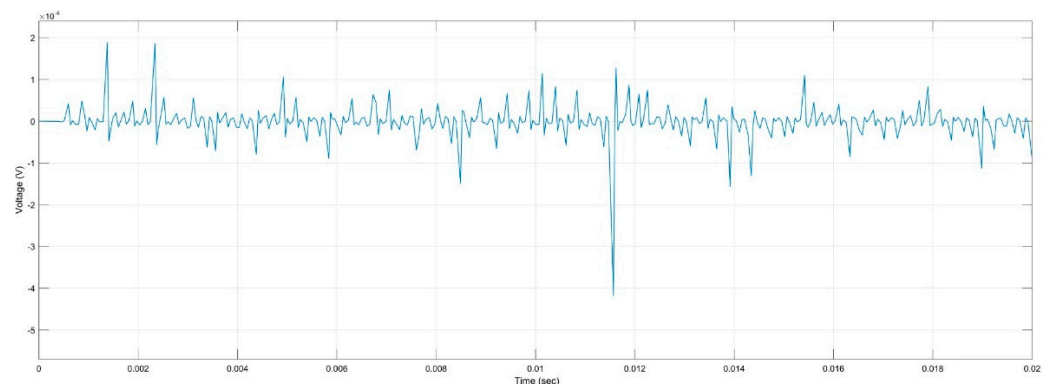


Figure 3. PD Activity for ER, 5 kV, h, r.

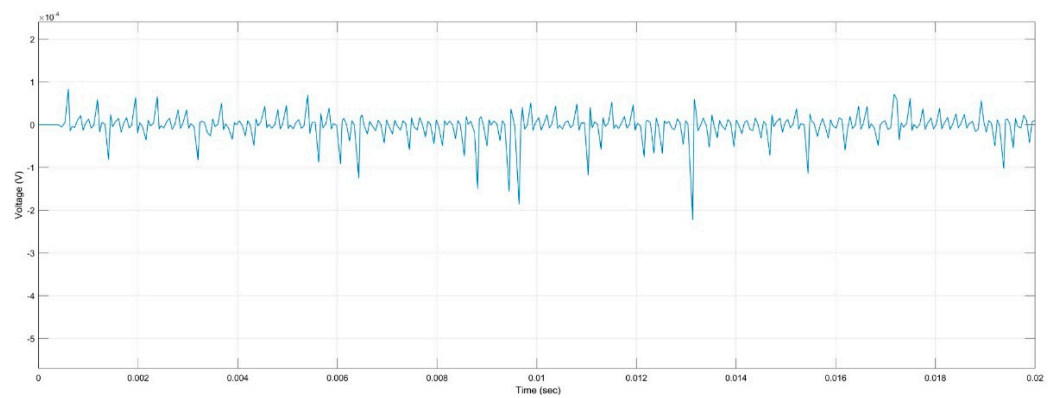


Figure 4. PD Activity for ER, 5 kV, h, 2 r.

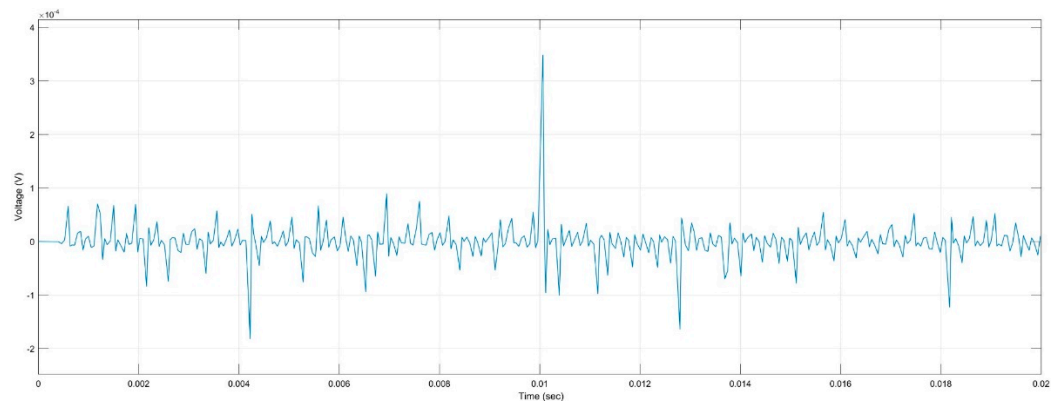


Figure 5. PD Activity for ER, 5 kV, 2 h, r.

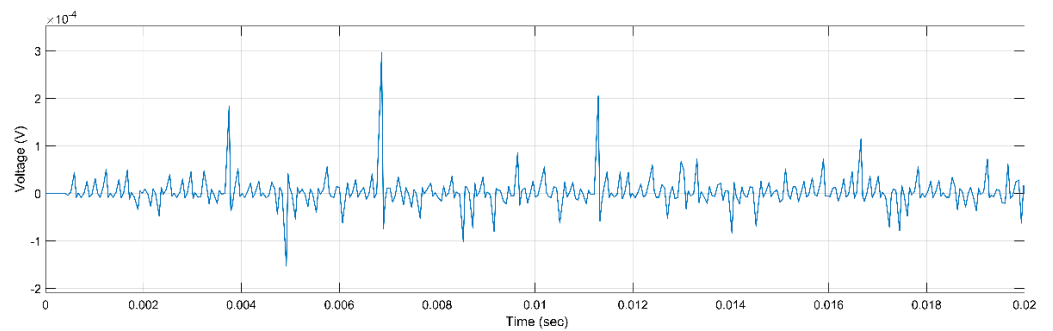


Figure 6. PD Activity for Mica, 5 kV, h, r.

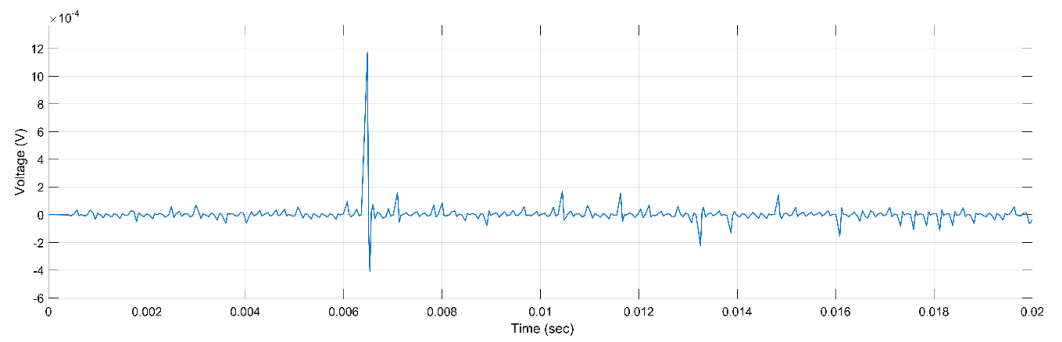


Figure 7. PD Activity for Mica, 10 kV, h, r.

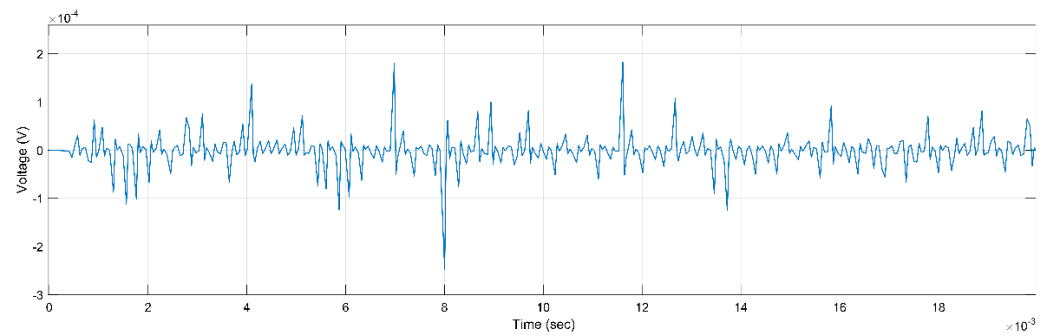


Figure 8. PD Activity for Mica, 15 kV, h, r.

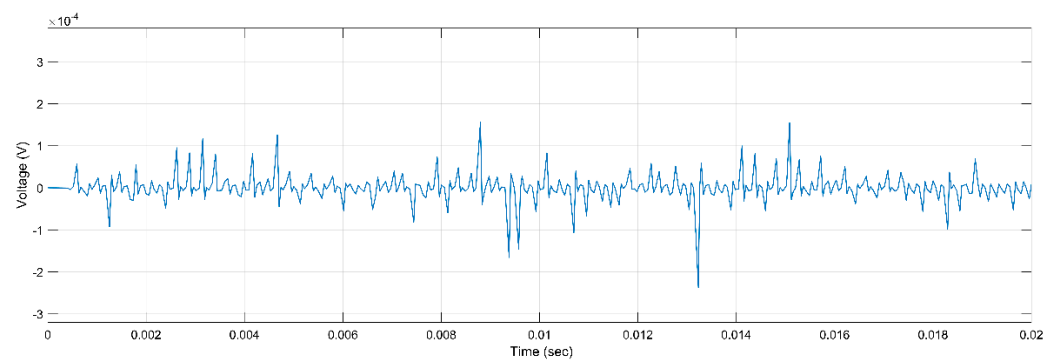


Figure 9. PD Activity for Combination, 5 kV, h, r.

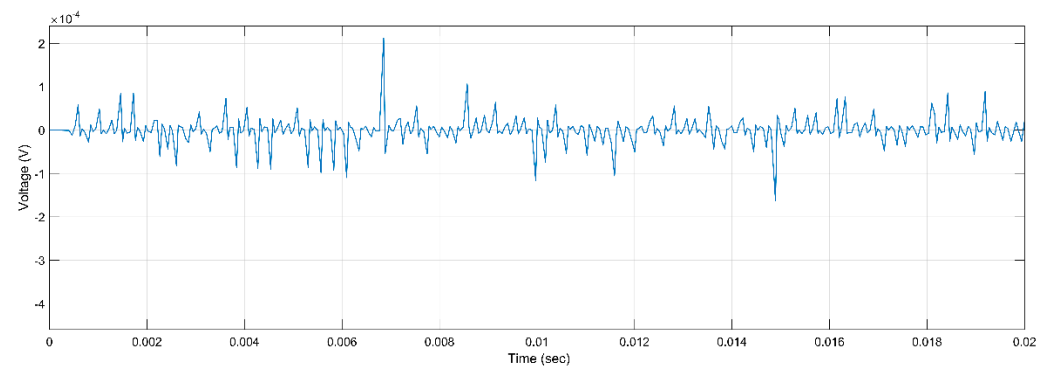


Figure 10. PD Activity for Combination, 10 kV, h, 2 r.

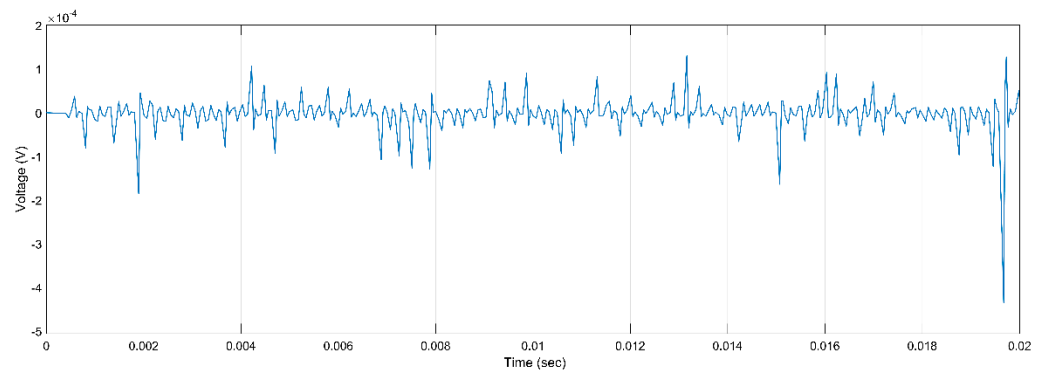


Figure 11. PD Activity for Combination, 15 kV, 2 h, r.

3.2. Capacitive Model with Resistors

This PD model is an advanced capacitive model, as resistors were placed opposite the three capacitors, as shown in Figure 12. The three resistors, R_a , R_b , and R_c , indicate the resistance of the insulation material, respectively, to the three capacitors C_a , C_b , and C_c . These resistors—which were added in order to have a more detailed representation of the insulation material, since geometric dimensions, relative permeability, and specific volumetric resistance are taken into account—are calculated by [15,16]:

$$R_a = \frac{\rho_{ins}h}{ab - \pi r^2} \tag{5}$$

$$R_b = \frac{\rho_{ins}(h - h_{cav})}{\pi r^2} \tag{6}$$

$$R_c = \frac{\rho_{cav}h_{cav}}{\pi r^2} \tag{7}$$

where ρ_{ins} is the electrical resistivity of solid insulation ($10^{15} \Omega m$), and ρ_{cav} is the electrical resistivity of the air cavity ($10^{15} \Omega m$).

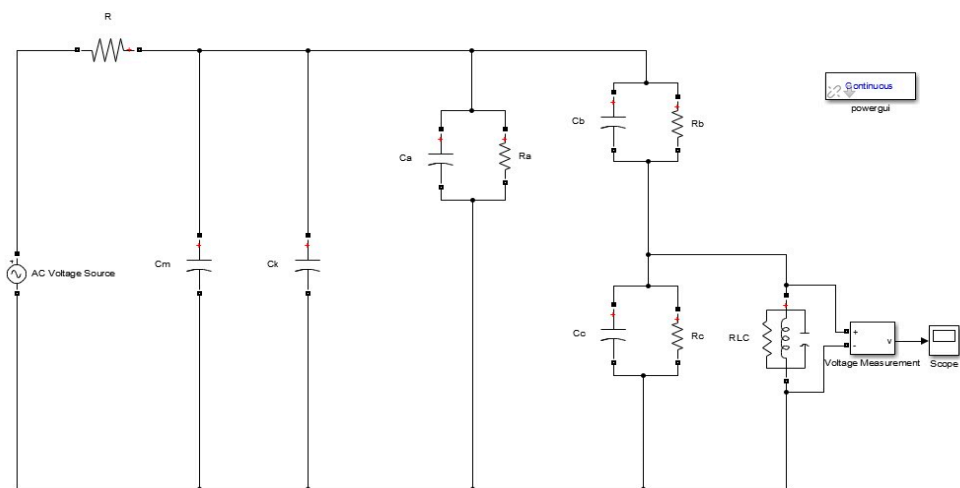


Figure 12. Capacitive resistance PD model.

Table 5 shows the values for the resistors added in this model for h and r. Table 6 presents the values for h and 2 r and Table 7 for 2 h and r. When the radius and the height increase, there is an increase in the values of R_b and R_c . The other parameters have the same values as those in the capacitive model.

Table 5. Capacitive–Resistor Model’s Parameters (h, r).

Parameter	Value
R_a	$5.8227 * 10^{-16} \Omega$
R_b	$2.1231 * 10^{-17} \Omega$
R_c	$1.4154 * 10^{-17} \Omega$

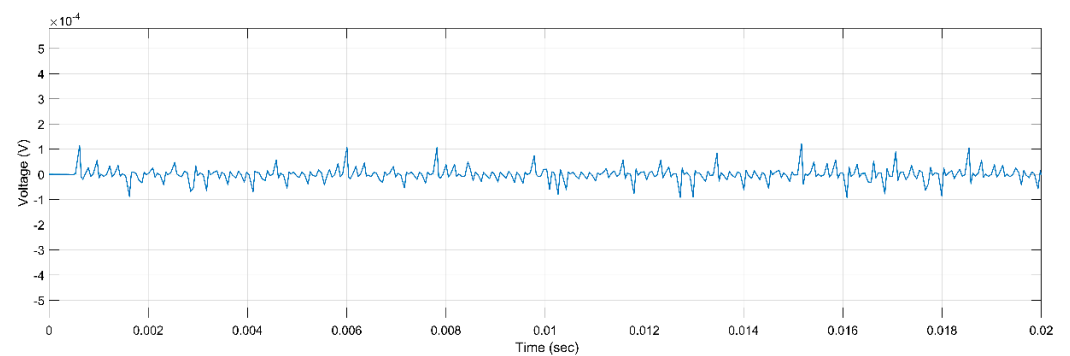
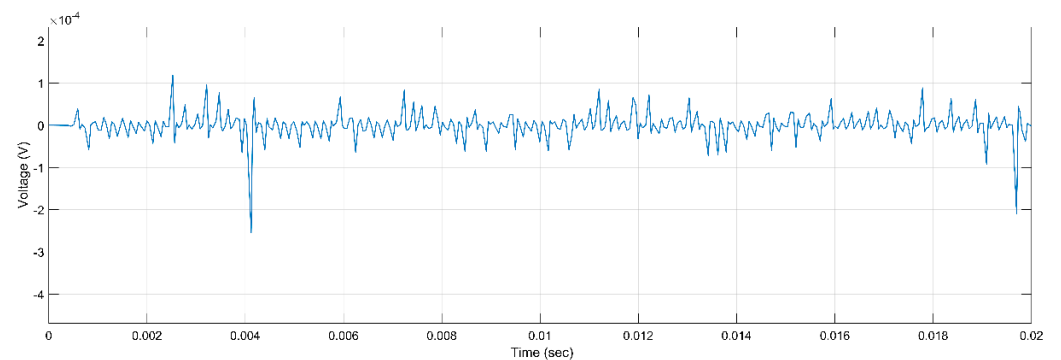
Table 6. Capacitive–Resistor Model’s Parameters (h, 2 r).

Parameter	Value
R_a	$1.1499 * 10^{-17} \Omega$
R_b	$5.3078 * 10^{-16} \Omega$
R_c	$3.5385 * 10^{-16} \Omega$

Table 7. Capacitive–Resistor Model’s Parameters (2 h, r).

Parameter	Value
R_a	$5.8227 * 10^{-16} \Omega$
R_b	$7.0771 * 10^{-16} \Omega$
R_c	$2.8308 * 10^{-17} \Omega$

A sample of the results of the second model is shown below (Figures 13–21). The results are similar to the corresponding diagrams of the first model in order to be more perceptible in comparison.

**Figure 13.** PD Activity for ER, 5 kV, h, r.**Figure 14.** PD Activity for ER, 5 kV, h, 2 r.

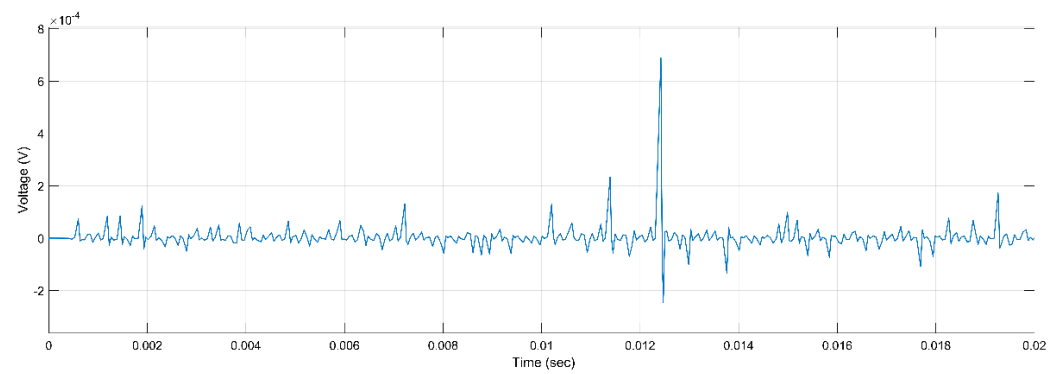


Figure 15. PD Activity for ER, 5 kV, 2 h, r.

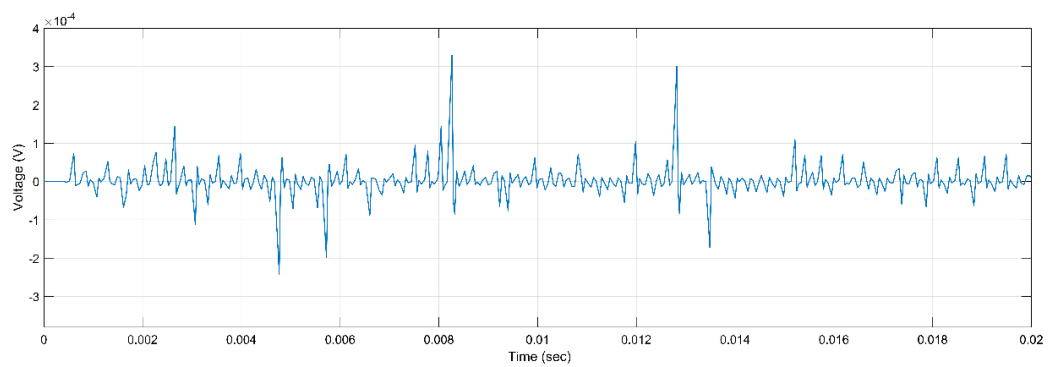


Figure 16. PD Activity for Mica, 5 kV, h, r.

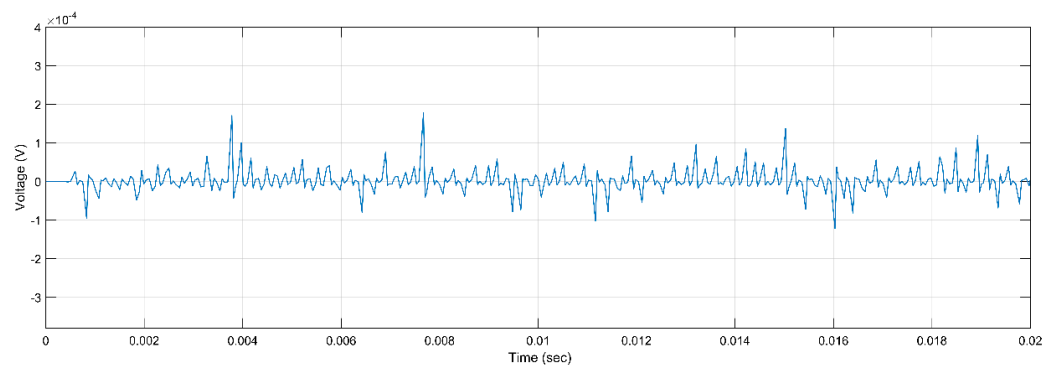


Figure 17. PD Activity for Mica, 10 kV, h, r.

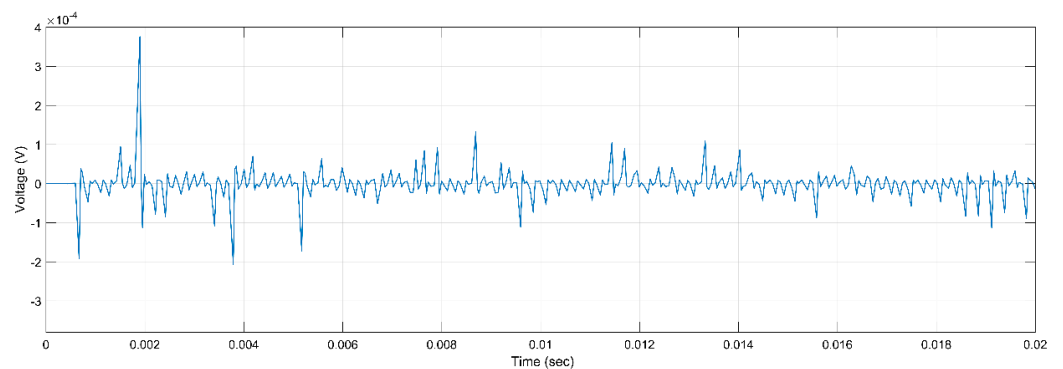


Figure 18. PD Activity for Mica, 15 kV, h, r.

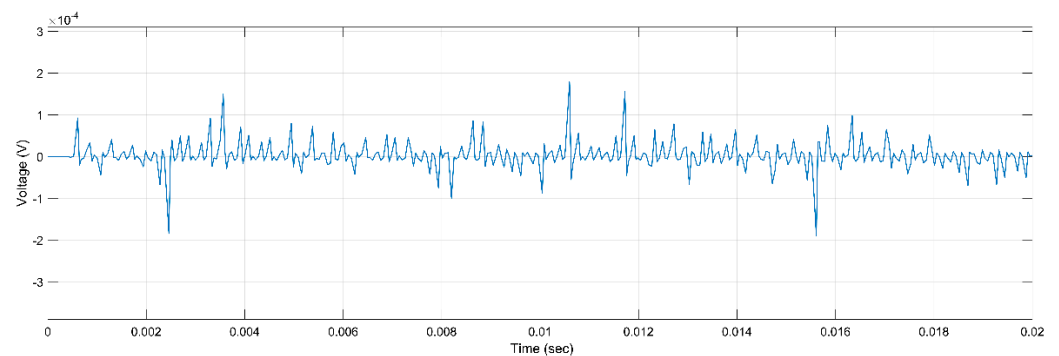


Figure 19. PD Activity for Combination, 5 kV, h, r.

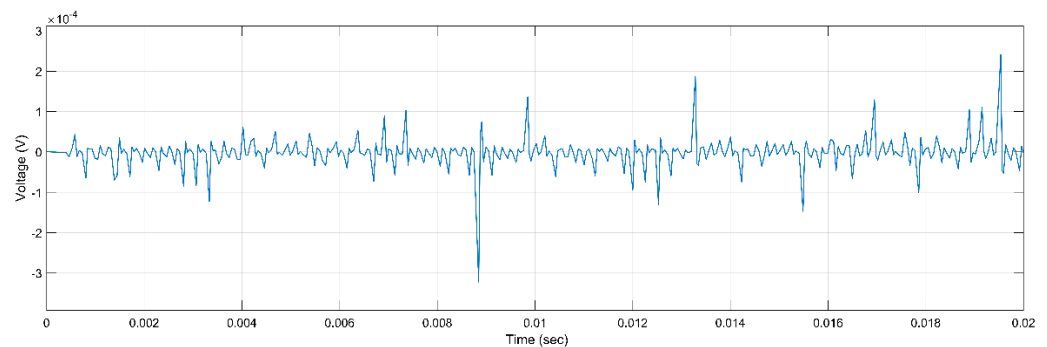


Figure 20. PD Activity for Combination, 10 kV, h, 2 r.

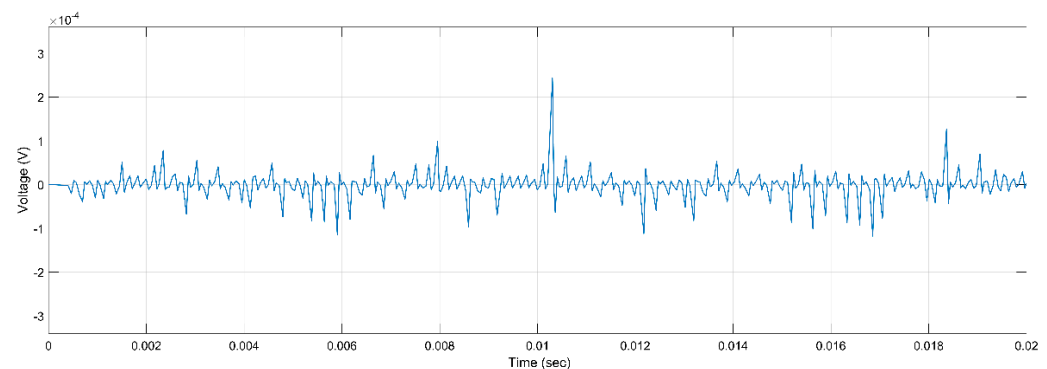


Figure 21. PD Activity for Combination, 15 kV, 2 h, r.

When the geometry of the void increases, either by increasing the radius or the height, the number of PDs increases, and the same happens when the applied voltage increases, as shown in the first model. As for the comparison between the three insulation materials, it is clear that the combination of the two materials seems to achieve the best results, while ER presents the fewest number of PDs and mica the smallest maximum PD amplitude.

3.3. Advanced Capacitive Model

The following Figure 22 shows an advanced model created in MATLAB/Simulink, which consists of capacitors and resistors. Besides them, new parameters have been included in this model [16,17]:

- A Resistor (R_{arc}), which is a linear resistance, indicating the resistance that the current has to face;
- A Breaker, which is connected with the voltage on the air cavity (V_c) and PD current (I_c). When the voltage becomes higher than the voltage on the air cavity, the breaker goes to state 1, and when the current becomes higher than PD current, the breaker goes to state 0.

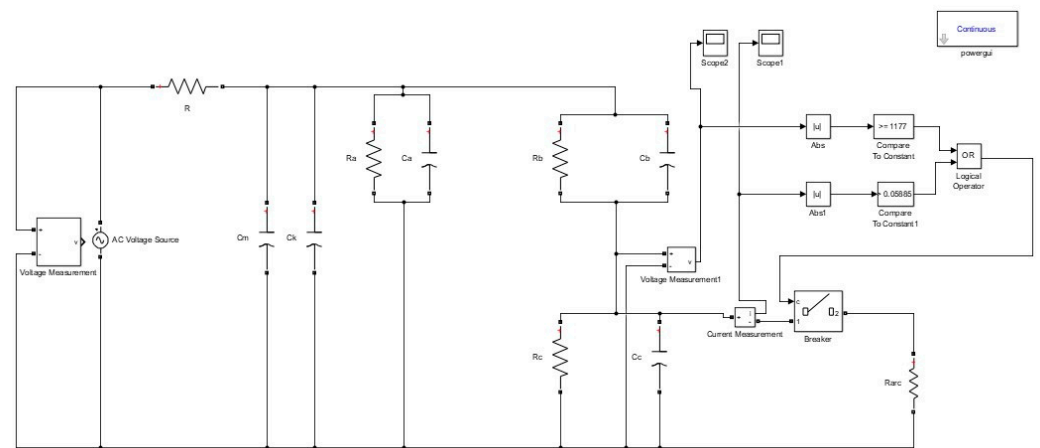


Figure 22. Advanced capacitive resistance PD model.

The following Table 8 shows the parameters of the aforementioned PD model, which were used for the different simulations. R_{arc} is the same for all simulations, but V_c and I_c change according to the geometries of the void. When the radius is doubled, there is no change in the values of V_c and I_c . However, when the height increases, there is a reduction in the values of V_c and I_c .

Table 8. Advanced Capacitive Model's Parameters.

Parameter	Value—r, h	Value—2 r, h	Value—r, 2 h
V_c	1.04639 kV	1.04639 kV	0.997 kV
I_c	0.05231 A	0.05231 A	0.04985 A
R_{arc}		10 k Ω	

The PD voltage is given by the empirical formula [16]:

$$V_c = 6.72\sqrt{\delta l} + 24.36(\delta l) \quad (8)$$

where $\delta = 1$ is the relative density of the air, and l is the gap length in cm. Moreover, when the PD is ignited, the current on the air void increases and decays gradually. The upper bound of the PD duration is 10 ns and this value corresponds to a decrease by half in the current, relative to the peak value, and that is why the current is calculated as half of the peak value.

Paschen's law gives the breakdown voltage for the start of an electrical discharge or electric arc as a function of the product of gas pressure and the gap distance between two electrodes. It applies for both enclosed cavities in solid insulation materials as well as gases, which are used as insulation materials [18].

Figures 23–31 show the results for the third model, presenting similar diagrams also selected for the previous two models. The difference in this model is that the diagrams are different due to V_c and I_c . The PDs are more visible in terms of their time and number. Apparent charge can be calculated by [16]:

$$q_a = \Delta V_c C_b \quad (9)$$

When the void increases either by increasing the height or the radius, the number of PDs increases. Moreover, the number of PDs increases when the applied voltage increases. The combination of the two insulation materials presents the lowest number of PDs, and mica seems to achieve the best results, while ER presents the fewest number of PDs and mica the maximum apparent charge, while ER the smallest.

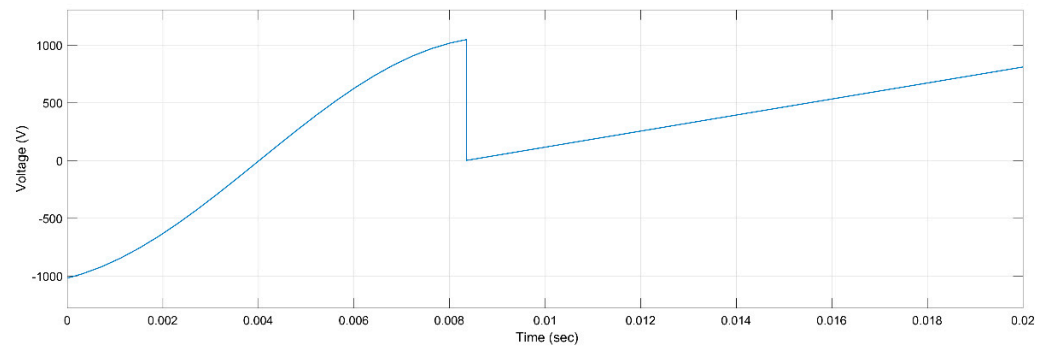


Figure 23. PD Activity for ER, 5 kV, h, r.

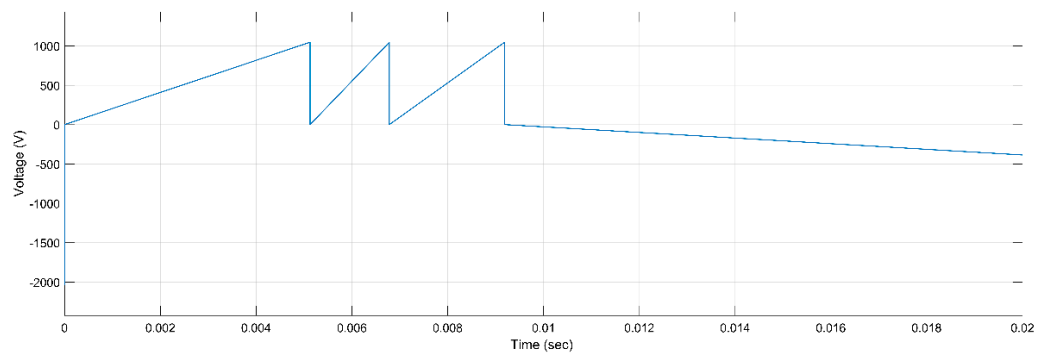


Figure 24. PD Activity for ER, 5 kV, h, 2 r.

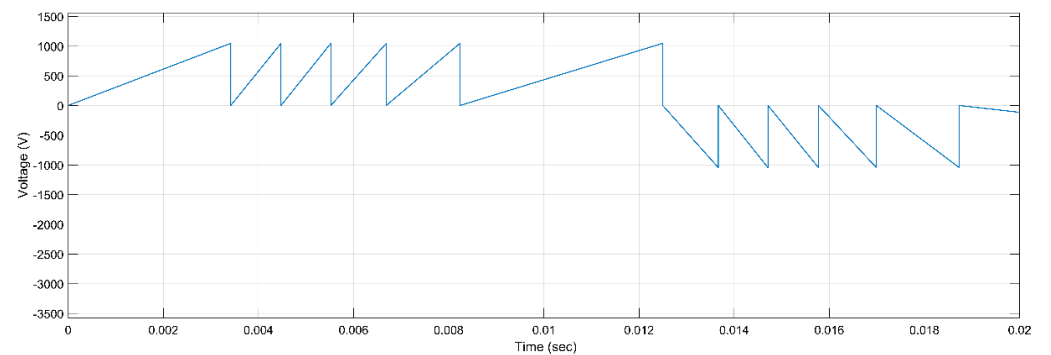


Figure 25. PD Activity for ER, 5 kV, 2 h, r.

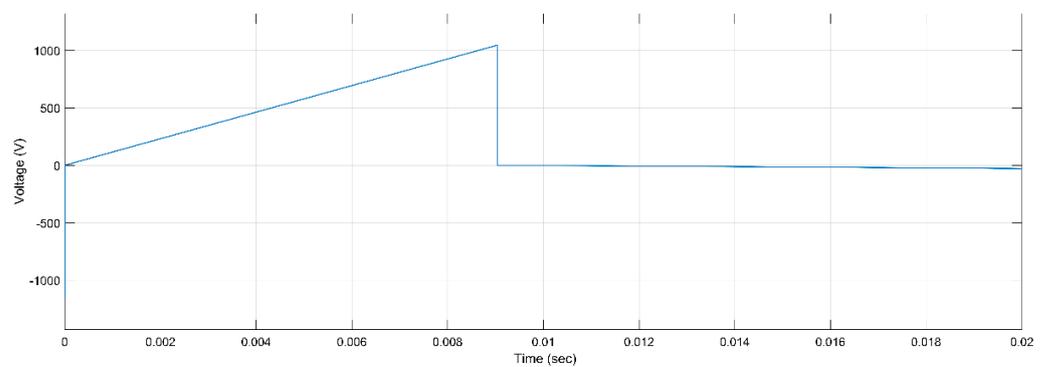


Figure 26. PD Activity for Mica, 5 kV, h, r.

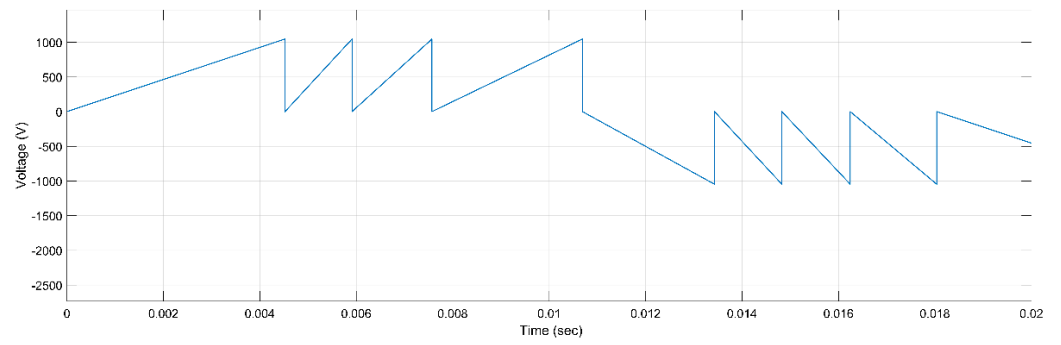


Figure 27. PD Activity for Mica, 10 kV, h, r.

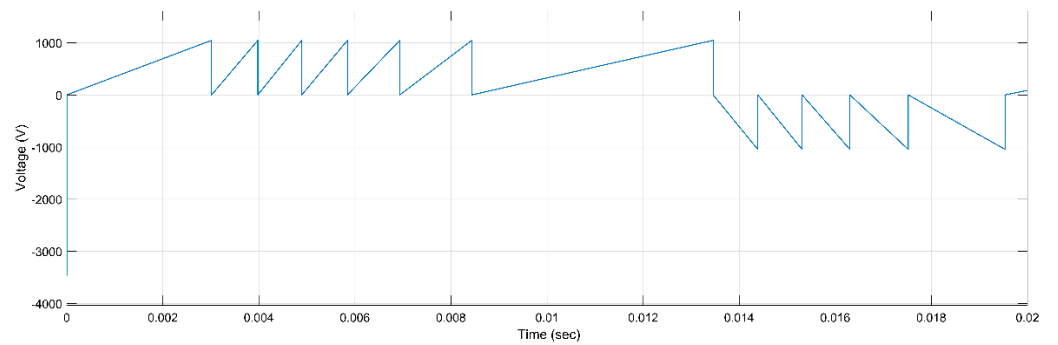


Figure 28. PD Activity for Mica, 15 kV, h, r.

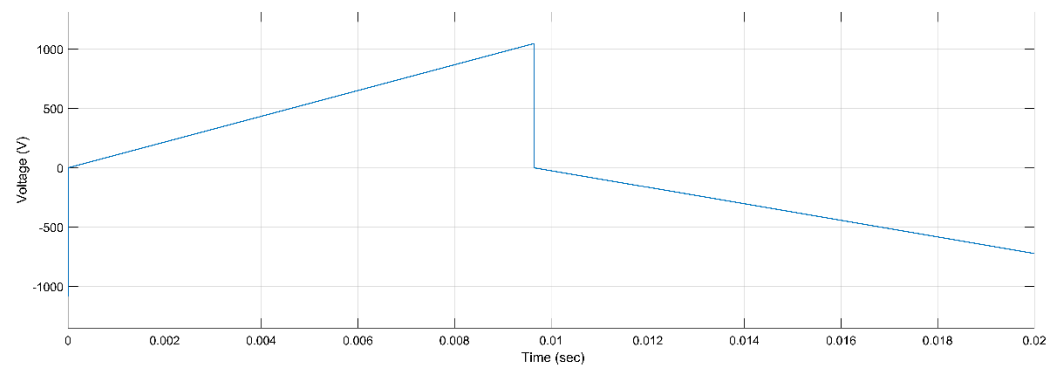


Figure 29. PD Activity for Combination, 5 kV, h, r.

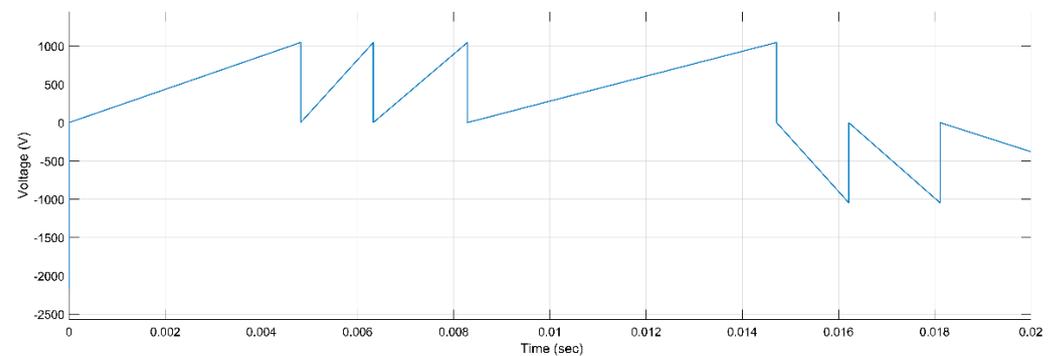


Figure 30. PD Activity for Combination, 10 kV, h, 2 r.

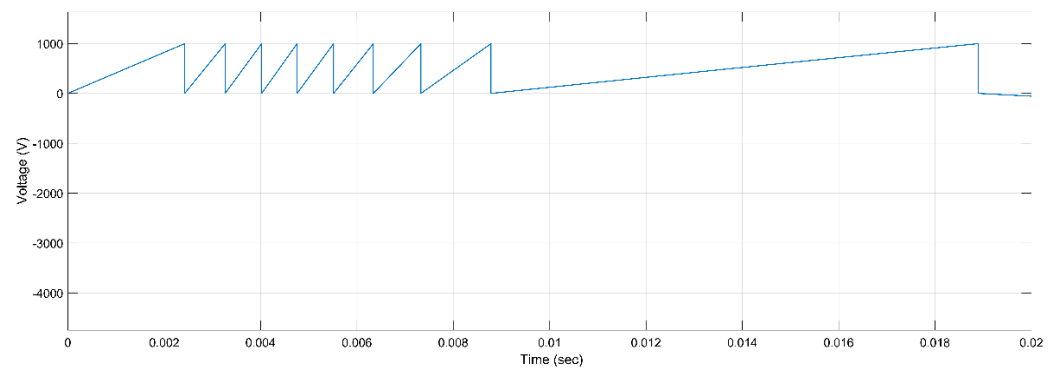


Figure 31. PD Activity for Combination, 15 kV, 2 h, r.

4. Discussion

The first PD model is the classic model created by Gemant and Philipoff, where three capacitances are used for representing the test object and a quite simple MI for detecting PDs. In the second model, three active spark resistances are connected in parallel with the three capacitances in order to more realistically represent the insulation material, while the MI is the same. A different approach to the PD activity is presented in the third model. V_c and I_c were used in order to calculate the number of PD pulses as well as the apparent charge and the true charge. Finally, the implementation of a breaker, operating according to certain conditions, was very important in order for the whole system to act more realistically. In addition, this model is characterized as an advanced PD model since the rate of signal decay and the moments of ignition and extinction of the spark are taken into consideration for studying PD activity [19–21].

As shown above, the authors decided to use the same applied voltages, void geometries, and insulation materials (ER, mica, and a combination of these two) in order for the results to be comparable. The above results apply to all simulations of each model used in the present study.

First of all, in most simulations, especially in the first two models, it is noted that when the applied voltage increases, the PD activity and the voltage amplitude of the PDs increase. The following Figure 32 presents some results from simulations of the third model with the same simulation parameters and different applied voltages, where it is obvious that when the voltage is 15 kV the number of PDs is greater than the number for 10 kV or 5 kV.

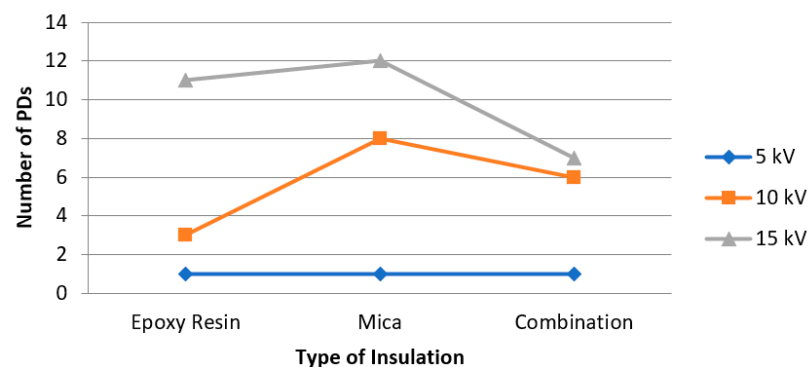


Figure 32. Number of PDs for the different insulation materials.

Additionally, by increasing either the height or the radius of the void, the PD activity is directly increased in all models. More specifically, the number of PDs in the ER and mica simulations increase more when the radius increases rather than when the height increases. The combination of the two materials presents the greatest number of PDs when the height increases. In most simulations, the PD activity increases more when the height of the void doubles rather than when the radius doubles.

Insulation materials play a vital role in PD activity. ER, mica, and the combination of these two materials were investigated. First of all, as we can see in Figures 33 and 34, in most simulations ER seems to present the largest PD amplitude, while the lowest is presented by mica. In most simulations, the lowest number of PDs is observed for the combination of the two materials. This is an important reason why it is preferred that the insulation system of many EMs, and especially SGs, is a combination of mica and ER. It is important to note that the following figures were created using data from simulations with the same parameters.

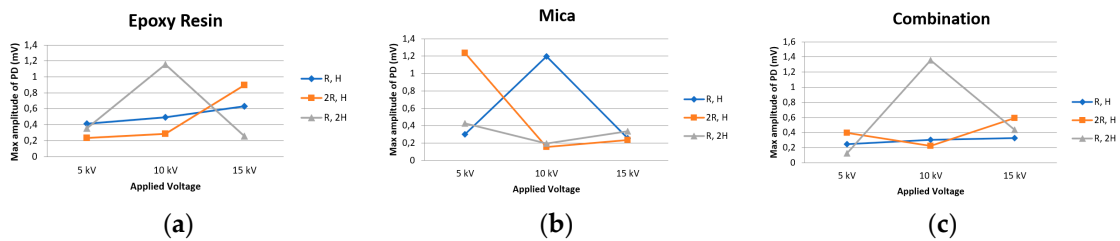


Figure 33. Maximum amplitude of PD for the 1st model for ER (a), mica (b), and combination (c).

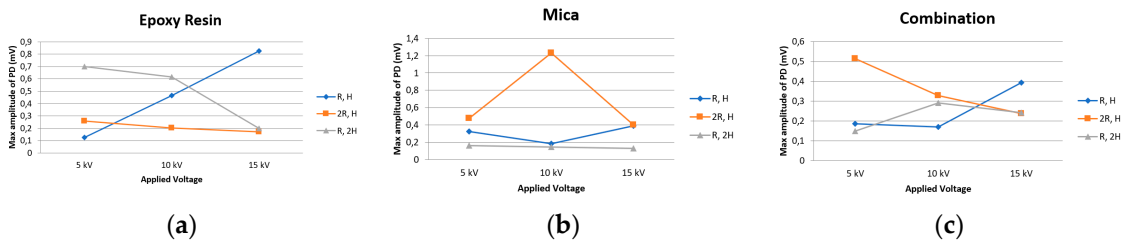


Figure 34. Maximum amplitude of PD for the 2nd model for ER (a), mica (b), and combination (c).

The results of the third model are quite different compared to these of the first two models, and they can be used for more direct conclusions. The difference in the simulation results is due to the use of V_c and I_c and the breaker. The number of PDs is more obvious in these figures. In most simulations, when the geometry characteristics of the void inside the insulation system increase, the number of PDs increases as well. Moreover, the increase in the height leads to more PDs than does the increase in the radius of the void.

The results of the third model can be used for calculating the apparent charge, as mentioned before. The following Figure 35 shows that, when the radius increases, the apparent charge increases more compared to the simulations where the height increases.

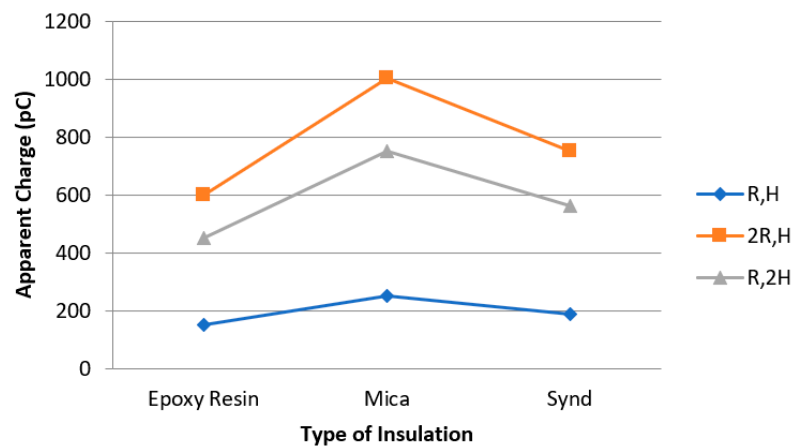


Figure 35. Apparent Charge for the Different Insulation Materials.

5. Conclusions

PDs are both a symptom of and a means for detecting the condition of the insulation of an EM, and that is why its measurement is very important. In this study, three different PD models were created and examined. The models are based on classic capacitive models and are mostly related to the Townsend mechanism, while Pedersen's model is related to the streamer mechanism. The authors chose to create these three models in order to investigate how the integration of the resistances and the use of the voltage on the air cavity (V_c) and PD current (I_c) affects the PD activity. Three different insulation materials (ER, mica, and the combination of these two materials), which are used the most in EM insulation systems, were studied due to having a significant enclosed void. The PD models studied in this manuscript, in order to examine PD activity in electrical machines, were adjusted by creating the test object and the enclosed void according to real conditions that could exist in a real electrical machine. The geometry of the void was changed either by increasing the height or the radius. In addition, three applied voltages were used. All the aforementioned factors were used in order to examine how the insulation materials were affected. The greater the applied voltage and the void's volume, the greater the PD activity and the number of PDs. Moreover, the insulation material that seems to have better behavior is the combination ER–mica, since it presents a reduction in the number of PDs in most of the simulations.

Different geometries of the void, applied voltages, and PD models can be used to extend this study, as well as the enhancement of these simulations with real experiments or data from real industrial EMs. Furthermore, these models can be used in order to create phase-resolved partial discharge (PRPD) diagrams, which in turn can be used as inputs for neural networks or other artificial intelligence (AI) models where, in combination with other results from different diagnostic techniques, such as insulation resistance (IR)/polarization index (PI) tests and power factor (PF)/dissipation factor (DF)/capacitance (C) tests, could create a more accurate predictive model for the condition of an EM. The future work of the authors will be aimed in this direction.

Author Contributions: Conceptualization, D.V., T.I., A.K., M.D. and J.-A.A.-D.; methodology, D.V., T.I., A.K., M.D. and J.-A.A.-D.; software, D.V. and T.I.; validation, D.V., T.I., A.K., M.D. and J.-A.A.-D.; formal analysis, D.V., T.I., A.K., M.D. and J.-A.A.-D.; investigation, D.V., T.I., A.K., M.D. and J.-A.A.-D.; resources, D.V., T.I., A.K. and M.D.; data curation, D.V. and T.I.; writing—original draft preparation, D.V., T.I., A.K., M.D. and J.-A.A.-D.; writing—review and editing, D.V., T.I., A.K., M.D. and J.-A.A.-D.; visualization, D.V., T.I., A.K., M.D. and J.-A.A.-D.; supervision, A.K., M.D. and J.-A.A.-D.; project administration, D.V., T.I., A.K., M.D. and J.-A.A.-D. All authors have read and agreed to the published version of the manuscript.

Funding: This research received no external funding.

Institutional Review Board Statement: Not applicable.

Informed Consent Statement: Not applicable.

Data Availability Statement: Not applicable.

Acknowledgments: The authors of this paper would like to thank Pericles Stratigopoulos, Director of Komotini Power Plant, Public Power Corporation S.A.—Hellas, for providing the pictures and the results of the PD measurements for this SG.

Conflicts of Interest: The authors declare no conflict of interest.

References

1. Chen, Y.; Zhao, Z.; Wu, H.; Chen, X.; Xiao, Q.; Yu, Y. Fault anomaly detection of synchronous machine winding based on isolation forest and impulse frequency response analysis. *Measurement* **2021**, *188*, 110531. [CrossRef]
2. National Center for Biotechnology Information. PubChem Compound Summary for CID 169944, Epoxy Resin. Available online: <https://pubchem.ncbi.nlm.nih.gov/compound/Epoxy-resin> (accessed on 19 January 2023).
3. Verginadis, D.; Karlis, A.; Danikas, M.G.; Antonino-Daviu, J.A. Investigation of Factors Affecting Partial Discharges on Epoxy Resin: Simulation, Experiments, and Reference on Electrical Machines. *Energies* **2021**, *14*, 6621. [CrossRef]

4. Wang, P.; Hui, S.; Akram, S.; Zhou, K.; Nazir, M.T.; Chen, Y.; Dong, H.; Javed, M.S.; Haq, I.U. Influence of Repetitive Square Voltage Duty Cycle on the Electrical Tree Characteristics of Epoxy Resin. *Polymers* **2020**, *12*, 2215. [[CrossRef](#)] [[PubMed](#)]
5. Da, Y.; Liu, J.; Gao, Z.; Xue, X. Studying the Influence of Mica Particles Size on the Properties of Epoxy Acrylate/Mica Com-posite Coatings through Reducing Mica Particles Size by the Ball-Milled Method. *Coating* **2022**, *12*, 98. [[CrossRef](#)]
6. Li, Z.; Zhang, Z.; Han, T.; Du, B.; Li, J.; Zhang, L. Effect of Harmonic Voltage on Partial Discharge Properties of LN2/PPLP Insulation for HTS DC Cable. *IEEE Trans. Appl. Supercond.* **2021**, *31*, 1–4. [[CrossRef](#)]
7. Moradnouri, A.; Vakilian, M.; Hekmati, A.; Fardmanesh, M. HTS Transformer's Partial Discharges Raised by Floating Particles and Nitrogen Bubbles. *J. Supercond. Nov. Magn.* **2020**, *33*, 3027–3034. [[CrossRef](#)]
8. Santos, M.G.; Braulio, G.A.; Bernardes, J.V.; De Salles, C.; Milanez, J.R.C.; Bortoni, E.C.; Bastos, G.S. Continuous Partial Discharges Analysis During Automated Thermal Cycle Aging Experiment. *IEEE Trans. Energy Convers.* **2020**, *35*, 1989–1992. [[CrossRef](#)]
9. Afrouzi, H.N.; Hassan, A.; Chee, D.T.Y.; Mehranzamir, K.; Malek, Z.A.; Mashak, S.V.; Ahmed, J. In-depth exploration of partial discharge modelling methods within insulations. *Clean. Eng. Technol.* **2022**, *6*, 100390. [[CrossRef](#)]
10. Cheng, G.; Pan, C.; Tang, J. Numerical Modeling of Partial Discharges in a Solid Dielectric-Bounded Cavity: A Review. *IEEE Trans. Dielectr. Electr. Insul.* **2019**, *26*, 981–1000.
11. Borghei, M.; Ghassemi, M.; Kordi, B.; Oliver, D. Modeling and Measurement of Internal Partial Discharges in Voids Artificially Made within 3D-Printed Pol-yactic Acid (PLA) Block. In Proceedings of the 2021 IEEE Electric Ship Technologies Symposium (ESTS), Arlington, TX, USA, 3–6 August 2021; pp. 1–6.
12. Vardakis, G.; Danikas, M.G.; Nterekas, A. Partial Discharge in Cavities and their Connection with Dipoles, Space Charges, and Some Phenomena Below Inception Voltage. *Eng. Technol. Appl. Sci. Res.* **2020**, *10*, 2869–5874. [[CrossRef](#)]
13. D'Amato, D.; Loncarski, J.; Monopoli, V.G.; Cupertino, F.; Di Noia, L.P.; Del Pizzo, A. Impact of PWM Voltage Waveforms in High-Speed Drives: A Survey on High-Frequency Motor Models and Partial Discharge Phenomenon. *Energies* **2022**, *15*, 1406. [[CrossRef](#)]
14. Philippe, R.; Jacques, N. *Materiaux de L'elektrotechnique*, 2nd ed.; Editions Georgi; PPUR Presses Polytechniques: Lausanne, Switzerland, 1979.
15. Verginadis, D.; Iakovidis, T.; Karlis, A.; Danikas, M.; Antonino-Daviu, J.-A. A Critical View on the Partial Discharge Models for Various Electrical Machines' Insulation Materials. *Eng. Proc.* **2022**, *24*, 12. [[CrossRef](#)]
16. Ignatev, N.I.; Silin, N.V.; Konfederatov, D.V. In Reference to the Simulation of Partial Discharges in Solid Dielectrics. In Proceedings of the 2020 International Multi-Conference on Industrial Engineering and Modern Technologies, Vladivostok, Russia, 6–9 October 2020.
17. Aakre, T.G.; Ildstad, E.; Hvidsten, S. Partial discharge inception voltage of voids enclosed in epoxy/mica versus voltage frequency and temperature. *IEEE Trans. Dielectr. Electr. Insul.* **2020**, *27*, 214–221. [[CrossRef](#)]
18. Lee, M.U.; Lee, J.; Lee, J.K.; Yun, G.S. Extended Scaling and Paschen Law for Micro-Sized Radiofrequency Plasma Breakdown. *Plasma Source Sci. Technol.* **2017**, *26*, 034003. [[CrossRef](#)]
19. Kumar, D.; Ranjana Singh, R., Dr. Simulation of Partial Discharge for Different Insulation Material Using MATLAB. *IJSRD-Int. J. Sci. Res. Dev.* **2015**, *3*, 660–663.
20. Gunawardana, S.D.M.S.; Kanchana, A.A.T.; Wijesingha, P.M.; Perera, H.A.P.B.; Samarasinghe, R.; Lucas, J.R. A Matlab Simulink Model for a Partial Discharge Measuring System. In *Electrical Engineering Conference*; University of Moratuwa: Sri Jayawardanapura Kotte, Sri Lanka, Katubedda, January 2015.
21. Credo, A.; Villani, M.; Popescu, M.; Riviere, N. Application of Epoxy Resin in Synchronous Reluctance Motors With Fluid-Shaped Barriers for E-Mobility. *IEEE Trans. Ind. Appl.* **2021**, *57*, 6440–6452. [[CrossRef](#)]

Disclaimer/Publisher's Note: The statements, opinions and data contained in all publications are solely those of the individual author(s) and contributor(s) and not of MDPI and/or the editor(s). MDPI and/or the editor(s) disclaim responsibility for any injury to people or property resulting from any ideas, methods, instructions or products referred to in the content.